

# Head-to-Head Coiled Arrangement of the Subunits of the Animal Fatty Acid Synthase

Andrzej Witkowski,<sup>1</sup> Alokesh Ghosal,<sup>1,4</sup>

Anil K. Joshi,<sup>1</sup> H. Ewa Witkowska,<sup>2</sup>

Francisco J. Asturias,<sup>3</sup> and Stuart Smith<sup>1,\*</sup>

<sup>1</sup>Children's Hospital Oakland Research Institute

5700 Martin Luther King Jr. Way

Oakland, California 94609

<sup>2</sup>Department of Stomatology

Biomolecular Resource Center Mass

Spectrometry Laboratory

University of California, San Francisco

San Francisco, California 94143

<sup>3</sup>The Scripps Research Institute

10550 North Torrey Pines Road

La Jolla, California 92037

## Summary

The role of the  $\beta$ -ketoacyl synthase domains in dimerization of the 2505 residue subunits of the multifunctional animal FAS has been evaluated by a combination of crosslinking and characterization of several truncated forms of the protein. Polypeptides containing only the N-terminal 971 residues can form dimers, but polypeptides lacking only the N-terminal 422 residue  $\beta$ -ketoacyl synthase domain cannot. FAS subunits can be crosslinked with spacer lengths as short as 6 Å, via cysteine residues engineered near the N terminus of the full-length polypeptides. The proximity of the N-terminal  $\beta$ -ketoacyl synthase domains and their essential role in dimerization is consistent with a revised model for the FAS in which a head-to-head arrangement of two coiled subunits facilitates functional interactions between the dimeric  $\beta$ -ketoacyl synthase and the acyl carrier protein domains of either subunit.

## Introduction

In plants and most prokaryotes, the enzymes required for the de novo biosynthesis of fatty acids from malonyl-CoA exist as discrete individual proteins (type II FASs), but, in animals, they are integrated into a single multifunctional polypeptide of 272 kDa that functions as a homodimer (type I FAS). Catalysis of the acyl chain-elongation reaction requires appropriate juxtaposition of the saturated acyl moiety, attached to the active site cysteine of the  $\beta$ -ketoacyl synthase, and the chain-extending malonyl moiety, attached to the 4'-phosphopantetheine arm of the acyl carrier protein (ACP). The monomeric form of the type I FAS is unable to catalyze this reaction, and discovery that the  $\beta$ -ketoacyl synthase active site cysteine of one subunit could be crosslinked by 1,3-dibromopropanone (DBP) to the

ACP phosphopantetheine of the companion subunit [1, 2] logically led to formulation of a model for the type I FAS in which two fully extended polypeptides are oriented head-to-tail, such that two sites for condensation are created at the subunit interface by direct juxtaposition of the  $\beta$ -ketoacyl synthase active site cysteine thiol of one subunit with the 4'-phosphopantetheine of the second subunit [3, 4]. This model, illustrated in cartoon form in Figure 1A, has enjoyed wide acceptance for 20 years; although, until recently, no serious attempt had been made to test its validity. We have applied several novel approaches to evaluate the model that involved (i) development of a system for the expression of fully active recombinant FAS in insect Sf9 cells; (ii) engineering of a panel of FAS mutants compromised in one or more of the functional domains; (iii) introduction of a double-tagging procedure that enabled us to engineer heterodimeric FAS containing different mutations on each subunit; (iv) engineering and characterization of a library of more than 30 such heterodimers to identify pairs of mutated subunits that were capable of complementing each other by producing an active heterodimeric FAS; (v) reexamination of the specificity of DBP crosslinking, taking advantage of our ability to construct FASs lacking either or both the  $\beta$ -ketoacyl synthase active site cysteine thiol (Cys161) and the 4'-phosphopantetheine thiol (at Ser2151) in one or both subunits; and (vi) engineering of a FAS heterodimer consisting of a wild-type subunit paired with a subunit compromised by mutations in all seven functional domains. In brief, our findings have revealed several serious inconsistencies with the classical head-to-tail model that collectively make a compelling case for the formulation of an alternative model that is consistent with biochemical and structural data. Thus, (i)  $\beta$ -ketoacyl synthase and malonyl/acetyl transferase domains interact functionally with ACP domains of both subunits even though, within each polypeptide, the phosphopantetheine moiety of the ACP domain is located more than 1500 residues distant from the active sites of these catalytic domains [5]; (ii) the dehydrase domain interacts exclusively with the ACP domain of the same subunit, even though these domains are separated by more than 1200 residues [5]; (iii) the phosphopantetheine thiol in the ACP domain can be crosslinked by a 5 Å spacer (DBP) with the  $\beta$ -ketoacyl synthase active site cysteine of either subunit [6]; and (iv) a heterodimeric FAS containing only one competent subunit is able to synthesize palmitic acid [7].

The proposed alternative model is illustrated in cartoon form in Figure 1B. A key feature of the classical model is the clear spatial separation of the two  $\beta$ -ketoacyl synthase domains that lie at opposite poles of the dimer. However, the  $\beta$ -ketoacyl synthases associated with the type II FASs are universally dimeric proteins in which the substrate binding pocket is comprised of residues from both subunits [8–12]. Although the  $\beta$ -ketoacyl synthase domains of type I FASs exhibit extensive sequence similarity, and likely share a common reaction mechanism with their type II counterparts [13], the pre-

\*Correspondence: ssmith@chori.org

<sup>4</sup> Present address: NIH, NICHD, LCMN, 35 Lincoln Drive, MSC 3712, PNRC Building 35, Bethesda, Maryland 20892.

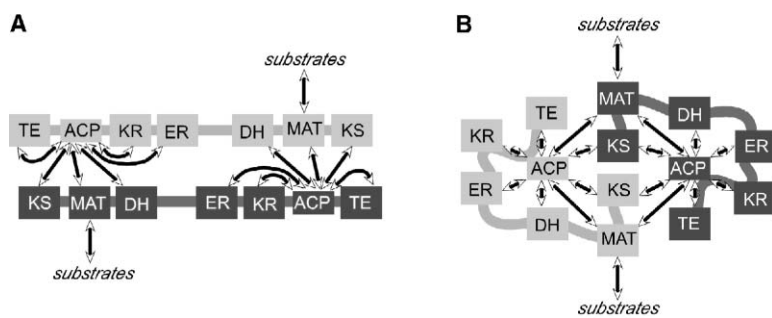


Figure 1. Cartoons Contrasting the Different Functional Contacts between Domains in the Classical Head-to-Tail Model and the Alternative Model

(A and B) The (A) classical model is adapted from [44], and the (B) alternative model is adapted from [5, 7]. In the classical model, functional contacts between  $\beta$ -ketoacyl synthase, malonyl/acetyl transferase and dehydrase domains, and the ACP occur exclusively across the subunit interface. KS,  $\beta$ -ketoacyl synthase; MAT, malonyl/acetyl transferase; DH, dehydrase; ER, enoyl reductase; KR,  $\beta$ -ketoacyl reductase; TE, thioesterase.

vailing head-to-tail model had precluded the possibility that within the type I FAS complex the two  $\beta$ -ketoacyl synthase domains engage in homodimeric interactions. Since the proposed alternative model does not disallow this possibility, we formulated an experimental approach designed to resolve this issue.

## Results

### Expression of the $\beta$ -Ketoacyl Synthase Domain of FAS

Several attempts were made to express the  $\beta$ -ketoacyl synthase domain separately from the multifunctional FAS polypeptide. Low-copy number plasmid constructs (pQE30) encoding residues 1–407 of the rat FAS (either as the “wild-type” sequence or as catalytically inactive mutants Cys161Ala or Lys326Ala), with and without N-terminal or C-terminal histidine tags, failed to generate significant amounts of soluble recombinant protein when transfected into *Escherichia coli*. Attempts to re-fold the  $\beta$ -ketoacyl synthase protein recovered in inclusion bodies were unsuccessful. Inclusion of 80 additional residues (1–487 FAS, see Figure 2) that have no counterpart in either the type II  $\beta$ -ketoacyl synthase or malonyl transferase proteins, and do not appear to be required for functioning of the adjacent malonyl/acetyl transferase domain [14], did not improve expression, neither did coupling of the  $\beta$ -ketoacyl synthase domain to glutathione transferase in a GST- $\beta$ -ketoacyl synthase chimera. Similarly, expression of the  $\beta$ -ketoacyl synthase domain in *Sf9* cells produced only small amounts of insoluble protein. As an alternative strategy to obtain an isolated  $\beta$ -ketoacyl synthase domain, we introduced a TEV protease cleavage site into the proline-rich linker region between the  $\beta$ -ketoacyl synthase and the malonyl/acetyl transferase domains in the context of a doubly tagged, N-FLAG, C-His<sub>6</sub> FAS (<sup>406</sup>PNTQQAPAPAP HAA was changed to <sup>406</sup>PNGPENLYFQ<sub>407</sub>GPHAA, (<sup>408</sup>tev)-FAS, Figure 2). This FAS retained full activity and could be completely cleaved between residues Q and G by the TEV protease to yield two fragments of ~200 and 50 kDa (Figure 3A, lanes 2 and 3). Confirmation of the identity of these species was provided by Western analysis: the ~50 kDa ( $\beta$ -ketoacyl synthase) was anti-FLAG positive, and the ~200 kDa species was anti-His<sub>6</sub> positive (details not shown). Cleavage by the TEV protease was accompanied by a loss in ability to catalyze the overall FAS reaction. Surprisingly, however, the  $\beta$ -ketoacyl synthase domain could not be separated from the large FAS fragment by either Ni-NTA or anti-

FLAG affinity chromatography of either the “nicked dimeric” or cold-dissociated “nicked monomeric” forms of the complex. This finding implied that, in the native polypeptide, the  $\beta$ -ketoacyl synthase domain maintains contacts with downstream domains both via its covalent linkage and via noncovalent interactions.

### Expression of the $\beta$ -Ketoacyl Synthase Domain Fused to Cognate FAS Domains

Based on the conjecture that noncovalent interactions between the  $\beta$ -ketoacyl synthase and adjacent domains might stabilize the  $\beta$ -ketoacyl synthase, we engineered two partial FAS constructs containing the N-terminal  $\beta$ -ketoacyl synthase domain and encompassing residues 1–809 and residues 1–971, which we anticipated as representing the first two and the first three catalytic domains, respectively (Figure 2). Both proteins were expressed in *Sf9* cells as N-His<sub>6</sub>-tagged proteins, purified and characterized. The 1–809 FAS construct, which expressed at very low levels (~1 mg/l culture medium), purified as a species with a molecular mass of ~93 kDa, as estimated by SDS-PAGE, which is close to the anticipated value of 88 kDa (Figure 3A, lane 6). High-performance gel filtration analysis revealed that the protein was exclusively monomeric (details not shown). The 1–809 FAS protein exhibited normal malonyl/acetyl transferase activity, but it lacked the  $\beta$ -ketoacyl synthase acyltransferase activity associated characteristically with the dimeric full-length FAS. The 1–971 FAS construct expressed at much higher levels (~10 mg/l) and purified as an ~110 kDa species, as estimated by SDS-PAGE, which is close to the anticipated value of 106 kDa (Figure 3A, lane 4). Gel filtration analysis revealed that the purified 1–971 FAS consisted of a mixture of three oligomeric species that exhibited elution volumes corresponding to ~82, 220, and 775 kDa (Figure 3B). Ageing of the mixture of oligomeric species for 7–8 days at 4°C in 20 mM phosphate buffer resulted in conversion of the higher-molecular mass forms to the species with an elution volume corresponding to ~82 kDa (Figure 3C). Upon restoration of the phosphate buffer concentration to 0.20 M and incubation at room temperature, the low-molecular mass species was converted to higher oligomers, predominantly the ~220 kDa species. Rechromatography of this ~220 kDa species on the gel filtration column further enhanced purity (Figure 3D). Based on a theoretical molecular mass value of 106 kDa for the 1–971 FAS polypeptide, the most plausible interpretation of these results is that the species corresponding to molecular masses of ~82 and

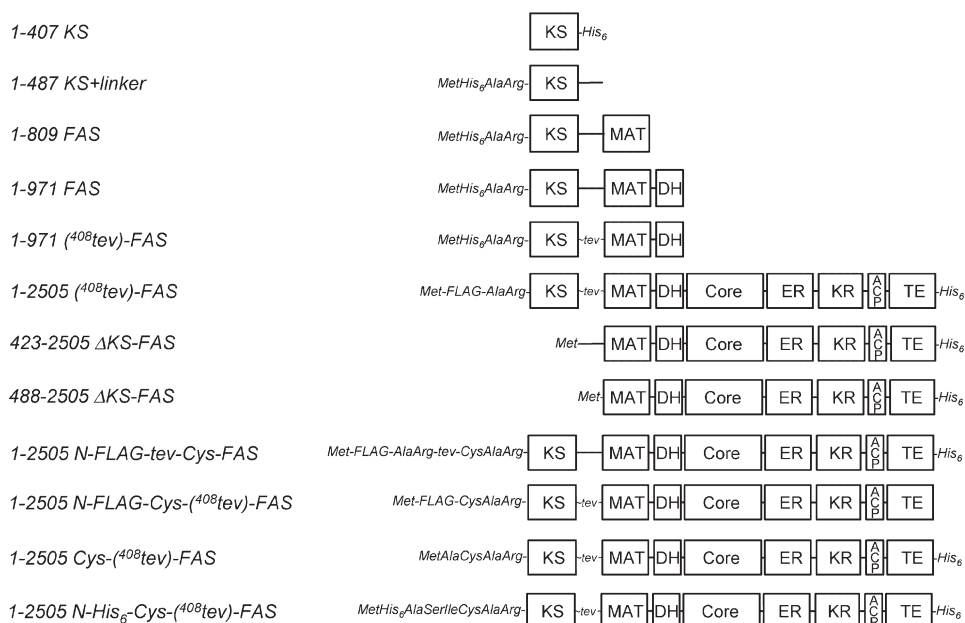


Figure 2. FAS Constructs Engineered for This Study

The numbering system is that of the wild-type rat FAS. His<sub>6</sub> and FLAG tags and TEV cleavage sites are not included in the numbering. For simplicity, the presence of C-terminal His-tag is not indicated in the construct annotation. The TEV recognition site was engineered into the proline-rich linker region ...<sup>406</sup>PNTQQAPAPAPHAALP... between the β-ketoacyl synthase and the malonyl/acetyl transferase domains in full-length FAS. Details of these constructions are available as [Supplemental Data](#).

220 kDa represent monomeric and dimeric forms and that the species corresponding to ~775 kDa represents a higher oligomer. The conditions used to effect dissociation of the oligomeric forms of the 1–971 FAS into the monomeric form (4°C, low salt concentration) and reassociation of the monomeric to the dimeric form (20°C, high salt concentration) are precisely the conditions that effect dissociation and reassociation of the full-length FAS [15]. In the case of the full-length FAS, dissociation and reassociation result in the loss and recovery of both overall FAS activity [15] and activity of the acyltransferase attributable to the β-ketoacyl synthase domain [16], but they do not affect the activity of the malonyl/acetyl transferase domain, when assessed with model substrates [16, 17]. These considerations prompted us to examine the partial activities associated with the oligomeric and dimeric forms of the 1–971 FAS. No significant dehydrase activity could be detected in either the monomeric or dimeric forms of the 1–971 FAS, suggesting that additional sequences beyond residue 971 may be required for this activity. The activity of the malonyl/acetyl transferase domain in the dimeric form of the 1–971 FAS protein, 2640 ± 78 U/mg assessed with model substrates, was unchanged upon dissociation and is similar to that reported previously for the isolated malonyl/acetyl transferase domain [14]. However, a striking difference was observed in the β-ketoacyl synthase-mediated acyltransferase activity of the dimeric (14.5 ± 0.12 U/mg) and monomeric (0.7 ± 0.01 U/mg) species. In comparison, the activities of the full-length FAS dimers and monomers are 6.9 and 0.2 ± 0.2 U/mg, respectively. Thus, the 1–971 FAS can be dissociated and reassociated with accompanying loss and restoration of the β-ketoacyl synthase-mediated

acyltransferase activity under the same conditions that produce a similar effect in the full-length FAS.

We attempted to isolate the β-ketoacyl synthase domain from the 1–971 FAS construct by engineering a TEV protease cleavage site between the β-ketoacyl synthase and malonyl/acetyl transferase domains (Figure 2, 1–971 (<sup>408</sup>tev)-FAS, as described above in the context of the full-length FAS. The protease recognition site in the 1–971 (<sup>408</sup>tev)-FAS protein, presented either as the dimer at 20°C or the monomer at 4°C, could be completely cleaved by TEV protease, as evidenced by SDS-PAGE (Figure 3A, lanes 4–5). Western analysis confirmed the identity of the proteolytic fragments: the ~50 kDa N-terminal β-ketoacyl synthase fragment was anti-His<sub>6</sub> positive, and the ~73 kDa C-terminal fragment was anti-His<sub>6</sub> negative (details not shown). Nevertheless, when the TEV-cleaved 1–971 (<sup>408</sup>tev)-FAS species were subjected to Ni-NTA affinity chromatography (the dimeric form at 20°C, the monomeric form at 4°C), both the N-His<sub>6</sub>-tagged β-ketoacyl synthase species and the untagged C-terminal fragment bound to the column and were co-eluted with 200 mM imidazole. These results demonstrated that, in the context of both the monomeric and dimeric forms of the 1–971 FAS, the β-ketoacyl synthase engages in strong noncovalent interactions with downstream regions.

#### Expression, Purification, and Characterization of a FAS Lacking the N-Terminal β-Ketoacyl Synthase Domain

To determine whether the presence of the β-ketoacyl synthase domains was essential for the formation of FAS dimers, we engineered two C-His<sub>6</sub>-tagged FASs lacking the N-terminal β-ketoacyl synthase domain

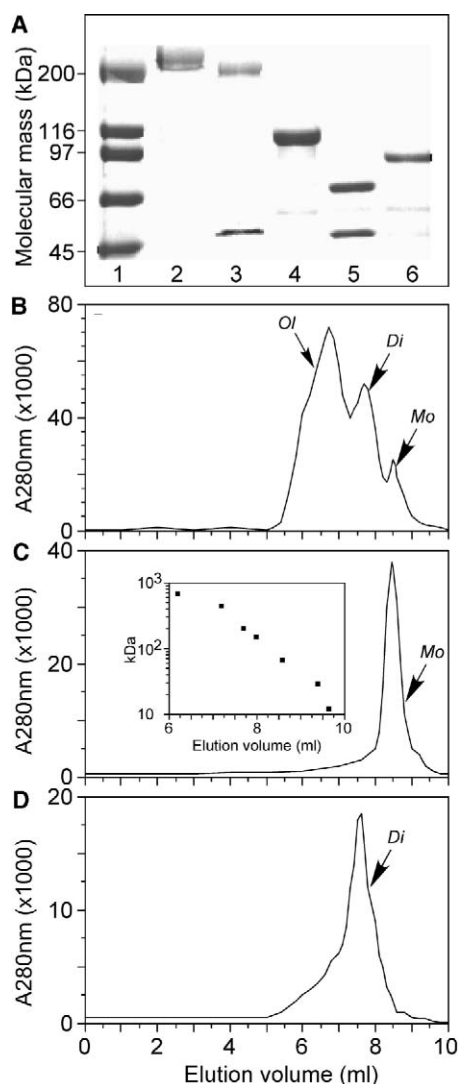


**Figure 3. Analysis of Full-Length and Partial FAS Proteins**  
(A) SDS-PAGE of: lane 1, molecular mass standards; lanes 2 and 3, 1–2505 (<sup>408</sup>tev)-FAS before and after cleavage, respectively; lanes 4 and 5, 1–971 (<sup>408</sup>tev)-FAS before and after cleavage, respectively; lane 6, 1–809 FAS.  
(B–D) Gel filtration profiles of 1–971 FAS preparations. (B) Original 1–971 FAS preparation. (C) Monomers produced by cold-induced dissociation (apparent Mr ~82 kDa, theoretical Mr 106 kDa). (D) Dimers produced by reassociation of monomeric species and purification by rechromatography (apparent Mr ~220 kDa, theoretical Mr 212 kDa). Insert, Mr standard plot. Ol, higher oligomers; Di, dimers; Mo, monomers.

and consisting of residues 423–2505 and 488–2505 (Figure 2,  $\Delta$ KS-FAS). The shorter construct lacked 64 residues from the long linker region between the  $\beta$ -ketoacyl synthase and the malonyl/acetyl transferase domains. Both constructs expressed well in Sf9 cells, and the proteins purified to homogeneity by anion exchange and Ni-NTA affinity chromatography had normal  $\beta$ -ketoacyl reductase activity. However, both truncated FAS constructs migrated exclusively as monomers on a gel filtration column and were significantly less thermally stable than the wild-type FAS (details not shown).

### Crosslinking of the N Termini of the $\beta$ -Ketoacyl Synthase Domains of Full-Length FAS

A survey of the crystal structures of type II  $\beta$ -ketoacyl synthase dimers revealed that the N-terminal residues of the two polypeptide chains typically are separated by 10–18 Å and are positioned on the surface of the protein. We reasoned that if this was also the case in type I FASs, then, provided an appropriate residue was located at the N termini, the two polypeptides likely could be crosslinked. To this end, we engineered various FAS cDNA constructs encoding a cysteine residue near the N terminus. The first of these constructs had encoded, near the N terminus, a cleavage site for either TEV or enterokinase proteases, with a cysteine residue at the position immediately following the cleavage site (Figure 2, 1–2505 N-FLAG-tev-Cys-FAS and 1–2505 N-FLAG-Cys-(<sup>408</sup>tev)-FAS, respectively). Our intention was to generate an N-terminal cysteine residue on each subunit by proteolytic cleavage and then to exploit the unique reactivity of the 1-amino, 2-thiol moieties at the N terminus for reaction with bis-thioester crosslinking reagents, by using a variation of the “native chemical ligation” reaction commonly used to couple large polypeptides [18, 19]. To our surprise, the introduction of a cysteine residue near the N terminus facilitated the crosslinking of the FAS subunits by low concentrations of bis-maleimido crosslinking reagents, obviating the need to generate an N-terminal cysteine residue by proteolysis. Approximately 98% of the crosslinked FAS migrated in the dimer fraction upon gel filtration, ruling out the possibility that interdimer crosslinking had occurred. Consequently, additional constructs were engineered to facilitate full exploitation of this finding (Figure 2, 1–2505 Cys-(<sup>408</sup>tev)-FAS and 1–2505 N-His<sub>6</sub>-Cys-(<sup>408</sup>tev)-FAS). The conditions employed for crosslinking via the engineered cysteine residues were optimized to minimize “nonspecific” crosslinking, as revealed in control experiments with the wild-type FAS. In all of these experiments, acetyl-CoA was included in the reaction mixture to acetylate the Cys161 and 4'-phosphopantetheine thiols and minimize the possibility that the reagents would introduce crosslinks between the  $\beta$ -ketoacyl synthase and the ACP domains. Using bis-maleimido-hexane at a concentration of only 80  $\mu$ M, all four constructs containing engineered cysteine residues could be crosslinked under conditions in which the wild-type FAS was relatively unaffected (Figure 4A, compare lanes 4–7 with lane 8). Furthermore, these constructs also could be crosslinked by reagents having shorter spacer elements, bis-maleimidobutane and bis-maleimidoethane (details shown for 1–2505 Cys-(<sup>408</sup>tev)-FAS, Figure 4A, lanes 2 and 3). Most significantly, a heterodimer consisting of one wild-type (N-His<sub>6</sub>-FAS) and one 1–2505 N-FLAG-Cys-(<sup>408</sup>tev)-FAS subunit was not crosslinked by bis-maleimido-hexane under these same conditions (Figure 4A, lane 9), revealing that a cysteine residue near the N terminus of both subunits was required to form the crosslink. The ranges of S-S distances that can be crosslinked by the ethane, butane, and hexane bis-maleimides have been estimated by stochastic dynamics simulations as 6.3–10.5, 4.5–14.1, and 3.5–15.6 Å, respectively [20], indicating that the cysteine residues engineered at the N termini of the two FAS subunits must be approximately 6.3–10.5 Å

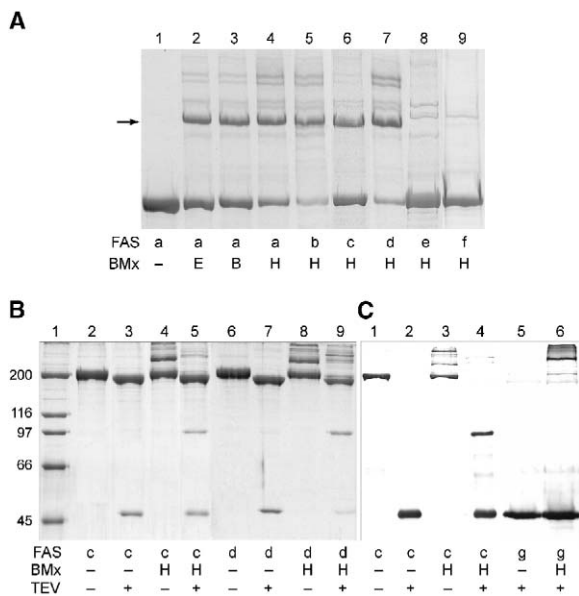


Figure 4. Electrophoretic Analysis of FAS Species Crosslinked at Engineered Cysteine Residues

(A) Various FASs were treated with different bis-maleimide (BMx) crosslinking reagents (E, ethane; B, butane; H, hexane) electrophoresed on 4% polyacrylamide gels and stained with Pro-Blue.

(B and C) FASs were treated with BMH and TEV protease, as indicated, electrophoresed on 7% polyacrylamide gels, and either stained with (B) Pro-Blue or (C) subjected to Western analysis with anti-FLAG antibodies. The positions of molecular mass standards are shown in lane 1 of (B). FAS species: a, 1–2505 Cys-(<sup>408</sup>tev)-FAS; b, 1–2505 N-FLAG-tev-Cys-FAS; c, 1–2505 N-FLAG-Cys-(<sup>408</sup>tev)-FAS; d, 1–2505 N-His<sub>6</sub>-Cys-(<sup>408</sup>tev)-FAS; e, 1–2505 N-His<sub>6</sub>-FAS; f, heterodimer of 1–2505 N-His<sub>6</sub>-FAS and 1–2505 N-FLAG-Cys-(<sup>408</sup>tev)-FAS (see the Supplemental Data for heterodimer isolation procedure); g, 1–2505 N-FLAG-(<sup>408</sup>tev)-FAS. The concentration of all crosslinkers in this experiment was 80 μM. The crosslinked species marked by the arrow in (A) accounted for 28%–37% of the total stained polypeptide species detected in the gel.

apart. Additional experiments revealed that DBP, which can crosslink thiols with a maximum spacing of 5.6 Å, could also generate a unique crosslinked species with FASs containing an engineered cysteine residue. This species is distinct from that formed by crosslinking of the Cys161 and 4'-phosphopantetheine thiols by DBP, as it was not formed from wild-type FAS (details not shown). Unequivocal evidence that the crosslinking involved the two N-terminal β-ketoacyl synthase domains was obtained by crosslinking the 1–2505 N-FLAG-Cys-(<sup>408</sup>tev)-FAS and the 1–2505 N-His<sub>6</sub>-Cys-(<sup>408</sup>tev)-FAS homodimers with bis-maleimido-hexane (Figure 4B, lanes 4 and 8); then, by exploiting the presence of the TEV protease cleavage site introduced between the β-ketoacyl synthase and the malonyl/acetyl transferase domains, the products were digested with TEV protease (Figure 4B, lanes 5 and 9). A distinct 90 kDa species that reacted positively to anti-FLAG antibodies in Western analysis could be detected in the digest (Figure 4C, lane 4), confirming that it was formed by the crosslinking of the N-terminally FLAG-tagged β-ketoacyl synthase domains within the context of the dimer. A control experiment, in which the same FAS species was sub-

jected to TEV protease digestion, without prior treatment with the crosslinker, yielded only an anti-FLAG-positive 45 kDa species corresponding to a single β-ketoacyl synthase domain (Figure 4C, lanes 1 and 2). N-FLAG-tagged FAS containing the <sup>408</sup>tev cleavage site but lacking the engineered cysteine residue generated exclusively the 45 kDa species upon treatment with bis-maleimido-hexane and TEV protease (Figure 4C, lanes 5 and 6).

Finally, the identity of the residues involved in forming the intersubunit crosslink was established by mass spectrometry. The N-His<sub>6</sub>-Cys-(<sup>408</sup>tev)-FAS was cross-linked with bis-maleimido-hexane or DBP, the reaction was quenched with mercaptoethanol, and the FAS was subjected to limited tryptic digestion and carboxyamidomethylated at cysteine residues. The His-tagged peptides were isolated by Ni-NTA affinity chromatography and were analyzed by MALDI-TOF MS. All four expected His-tagged peptides were identified. The smallest peptide, MH<sup>+</sup> 1185.697 Da, was matched to the tryptic peptide EGASH<sub>6</sub> (expected MH<sup>+</sup> 1185.505 Da) derived from the C terminus of FAS. The second peptide, MH<sup>+</sup> 1673.04, was matched to the N-acetylated, carboxyamidomethylated N-terminal tryptic peptide MH<sub>6</sub>ASICAR (expected MH<sup>+</sup> 1672.745 Da). The third peptide, MH<sup>+</sup> 1970.181 Da, corresponded to the same N-terminal tryptic peptide in which the cysteine residue had been reacted with BMH and the second maleimido group had been reacted with mercaptoethanol in the quenching step (expected MH<sup>+</sup> 1969.847 Da). Most importantly, the fourth peptide, MH<sup>+</sup> 3506.757 Da, corresponded to a pair of N-terminal tryptic peptides linked with a bis-maleimido-hexane moiety between the two cysteine residues (expected MH<sup>+</sup> 3506.549 Da, Figure 5A). Similarly, reaction of FAS with DBP generated three products, 1185.645, 1673.005, and 3284.726 Da, corresponding to the C-terminal, the carboxyamidomethylated N-terminal, and the crosslinked N-terminal peptides, respectively (expected MH<sup>+</sup> 1185.505, 1672.745, and 3284.450 Da); the spectrum for the crosslinked N-terminal peptides is shown in Figure 5B.

The sequence of N-terminal tryptic peptides cross-linked with bis-maleimido-hexane and DBP was examined by LC ESI MS/MS (Figure 5C and Supplemental Data available with this article online, respectively). MS/MS spectra of the crosslinked peptides are dominated by cleavages within the His-tag portion of their sequences. In addition to y and b ions, intense internal ions derived from the H<sub>6</sub> portion of the tag are also observed (for details, see DBP data in the Supplemental Data). With the exception of the y<sub>1</sub> ion, all other observed y ions encompass the crosslink site (Cys11-Cys11) and are consistent with the crosslinker still attached to both anchoring sites. As expected, the crosslinker itself is relatively stable under conditions of MS/MS. Due to the isobaric nature of product ions derived from cleavages at various positions within two identical MHHHHHH sequences present in the crosslink peptide, many of the observed ions are likely to represent mixtures of discrete MS/MS products. Nevertheless, these ambiguities do not affect the conclusions that can be drawn about the identity and sequence of the crosslinked peptide species. In conclusion, the mass fragmentation data establish unequivocally that both bis-

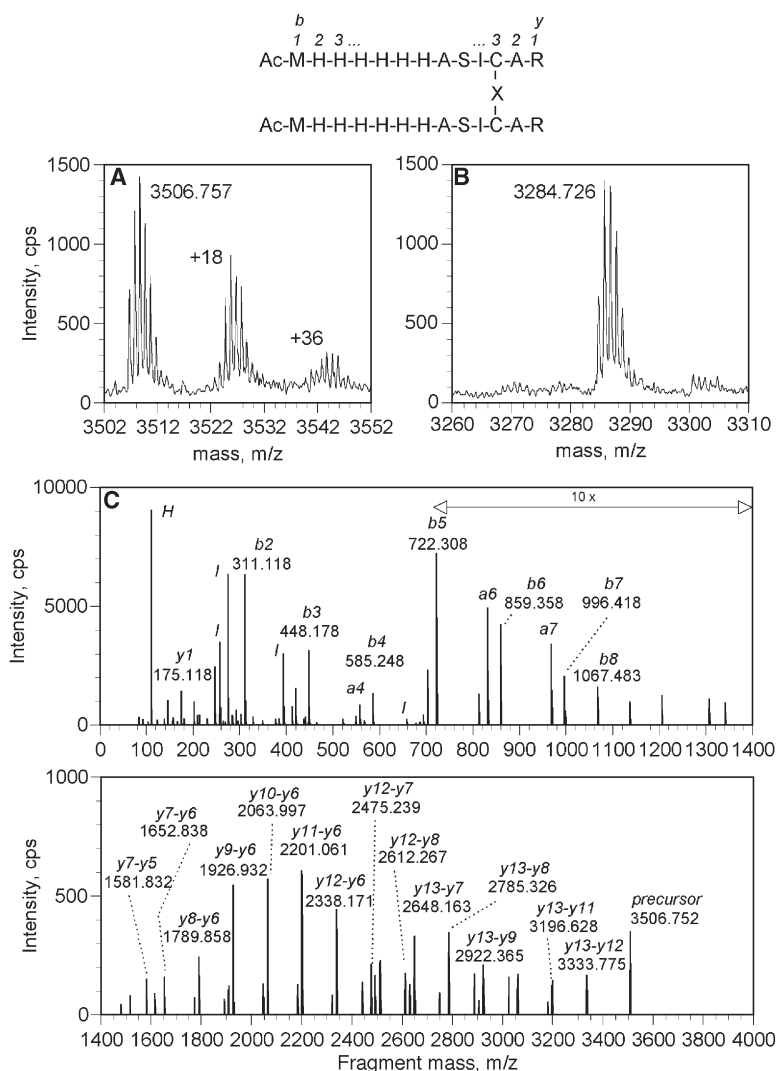


Figure 5. Verification by Mass Spectrometry that Cysteine Residues Engineered at the N Termini of FAS Can Form an Intersubunit Crosslink

(A–C) Homodimeric 1–2505 N-His<sub>6</sub>-Cys-(<sup>408</sup>tev)-FAS was treated with either (A and C) BMH or (B) DBP and digested with trypsin, and the N-terminal His-tagged peptides were isolated and analyzed by either (A and B) MALDI-TOF MS or (C) ESI Tandem MS. The sequence of the crosslinked peptide, together with annotations of ions, is shown above the spectra; the crosslinker moiety attached to the two cysteine thiols is shown as “X.” (A and B) For the MALDI-TOF MS, experimental monoisotopic MH<sup>+</sup> masses are shown above the spectra; corresponding expected masses for N-terminal peptides of FAS dimer crosslinked with BMH and DBP are 3506.549 and 3284.450 Da, respectively. In (A), mass increments of 18 and 36 Da represent products of hydrolysis of one and both N-alkyl succinimidyl moieties to N-alkyl succinimic acid. For clarity of presentation, in (C), an original ESI tandem mass spectrum was deconvoluted to a zero charge state and then redrawn to show fragment ions as singly charged species. Annotation of fragment ions follows the established nomenclature [45]. Thus, *b*, *y*, and *I* denote N-terminal, C-terminal, and internal fragments, respectively; symbols *y*-*y* present crosslinked fragments; *H* is a His immonium ion, and *a* = *b* – 28 Da. The –28 ion as well as the –17 and –18 Da ions are commonly produced upon fragmentation of peptides. Most of the –17 Da, –18 Da, and internal ions are not annotated. When several possible crosslinked fragments have identical predicted *m/z*, only the one combining the longest and shortest sequences within two identical counterparts of the precursor ion is shown. The double-headed arrow in (C) marks a portion of the spectrum shown with 10-fold amplification of intensity scale (*y* axis).

maleimido-hexane and DBP are capable of forming intersubunit crosslinks between the cysteine residues engineered at the N termini of the  $\beta$ -ketoacyl synthase domains.

## Discussion

Our inability to express the  $\beta$ -ketoacyl synthase domain of FAS as a freestanding protein, or to recover the domain following proteolytic cleavage from either full-length or truncated forms of FAS, necessitated the development of alternative strategies to evaluate the possibility that this domain might engage in homodimeric interactions critical for the functioning of the complex.

Dimers formed by the 1–971 FAS, which are active in the  $\beta$ -ketoacyl synthase-catalyzed acyltransferase reaction, can be converted to monomers by cold-induced dissociation in low-ionic strength buffer and reassociated to dimers by rewarming in high-ionic strength phosphate. The monomer to dimer transition is accompanied by restoration of  $\beta$ -ketoacyl synthase acyltransferase activity. These are exactly the same conditions that effect

dissociation and reassociation of full-length FAS subunits, indicating that structural elements within the first 971 residues may play a role in the maintenance of the dimeric form of the FAS. The inability of the 1–809 FAS to dimerize suggested that perhaps both the  $\beta$ -ketoacyl synthase and the dehydrase domains are involved in stabilizing the FAS dimer. In type II FAS systems,  $\beta$ -ketoacyl synthase [21] and dehydrase [22, 23] proteins are dimeric, whereas the malonyl transferase is monomeric [24, 25]. Further experiments focused specifically on the role of the  $\beta$ -ketoacyl synthase domain in dimerization, and, significantly, two FASs lacking the entire N-terminal  $\beta$ -ketoacyl synthase domain (488–2505 and 423–2505  $\Delta$ KS-FASs) were both found to be entirely monomeric and significantly less thermally stable than the full-length wild-type FAS. These properties are very similar to those reported previously for a FAS mutant in which the  $\beta$ -ketoacyl synthase active site cysteine residue had been replaced with threonine [26]. Thus, for the FAS to form dimers, the  $\beta$ -ketoacyl synthase domains must be present, and the integrity of the active site region must be preserved.

Direct evidence indicating that the  $\beta$ -ketoacyl domains might be close enough to form dimers was sought by using a crosslinking approach in which a new cysteine residue was introduced near the N terminus of the FAS (position -3). Indeed, the two polypeptides of these mutant FAS dimers could be readily crosslinked by DBP and bis-maleimide reagents with spacer distances as short as  $\sim 6$  Å. Compelling evidence was obtained indicating that the crosslinking involves the engineered cysteine thiols at the N termini of the two polypeptides. Thus, following treatment with the crosslinking reagents, proteolytic cleavage at a TEV recognition site introduced immediately downstream of the  $\beta$ -ketoacyl synthase domain revealed that the two N-terminal domains had been crosslinked. Crosslinking was not observed in a heterodimer that contained an engineered cysteine residue in only one subunit. Furthermore, crosslinking was observed with four fully active FAS species that contained sequences of different lengths and composition upstream from the engineered cysteine residue. Therefore, we regard it as highly unlikely that the proximal positioning of the two N termini represents an artifact produced by a structural rearrangement of the dimer brought about by the introduction of a specific unnatural sequence at the N termini. Conclusive evidence verifying that the bis-maleimide and DBP reagents introduce an intersubunit crosslink via the cysteine residues engineered at the N termini was obtained by mass spectrometric analysis.

These experiments provide irrefutable evidence that the N termini of the two  $\beta$ -ketoacyl synthase domains of the type I FAS dimer are located close together. It seems highly likely then that the N-terminal  $\beta$ -ketoacyl synthase domains are in fact homodimeric. Indeed, it is possible to model the  $\beta$ -ketoacyl synthase domain as a dimer based on the known crystal structures of the freestanding type II counterparts (Figures 6A and 6B). Furthermore, each of the crosslinkers used to ligate the cysteine residues engineered at position -3 can be accommodated in the structure. The structure of the N-terminal region containing the propanone crosslinker is shown in Figure 6C.

Recent single-particle analysis of electron micrographs of N-terminally His<sub>6</sub>-tagged FAS decorated with Ni-NTA nanogold have revealed that the gold clusters are localized exclusively near the center of the FAS dimer (F.J.A., J.Z. Chadick, I.K. Cheung, H. Stark, A.W., A.K.J., and S.S., unpublished data). Collectively, these findings indicate that the two N-terminal  $\beta$ -ketoacyl synthase domains of the FAS are homodimers and are positioned near the center of the dimer.

In summary, there is now a substantial body of evidence indicating that the  $\beta$ -ketoacyl synthase domains of the animal FAS function as a homodimer and play a significant role in stabilizing the dimeric form of the complex. Thus, (i) activity of the partial reactions of the  $\beta$ -ketoacyl-synthase—acyl chain transfer to the active site cysteine, decarboxylation of malonyl moieties to form the active carbanion species, and condensation of the substrates to form the  $\beta$ -ketoacyl moiety—all require the dimeric form of the FAS [13, 27]; (ii) FASs carrying certain single residue mutations in the active site region of  $\beta$ -ketoacyl synthase (Cys161Thr and Lys326Leu) fail to form stable dimers [28]; (iii) FAS lack-

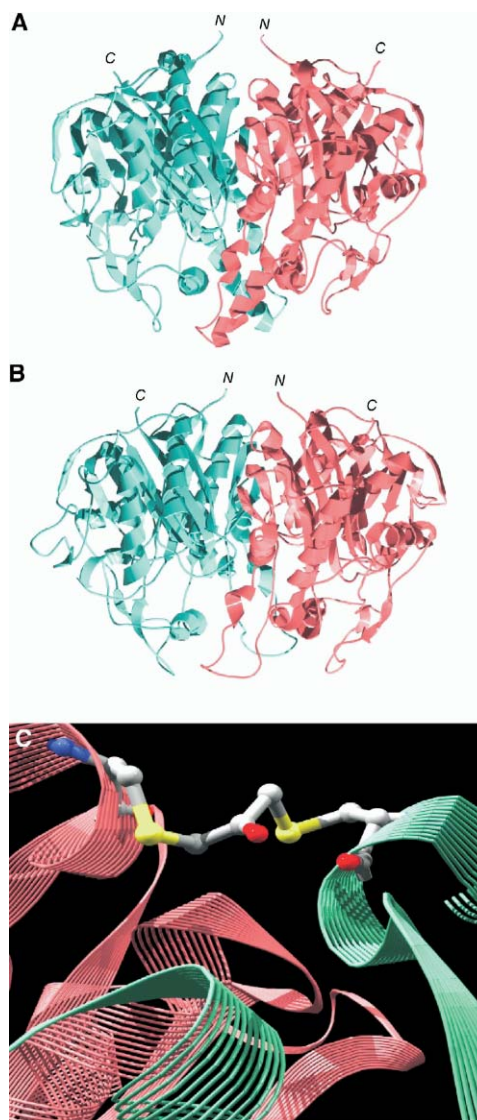


Figure 6. Homology Modeling of the  $\beta$ -Ketoacyl Synthase Domain of FAS

(A and B) Ribbon presentation of the X-ray structure of *Streptococcus pneumoniae* KAS II and a model of  $\beta$ -ketoacyl synthase domain of FAS, respectively. The subunits are distinguished by blue and red coloring.

(C) View of an N-terminally modified model of the  $\beta$ -ketoacyl synthase domain crosslinked with 2-propanone; compared with that in (B), the view is rotated 180° about the vertical axis in the plane of the paper. The MACAR peptide was attached to the N-terminal methionine of the  $\beta$ -ketoacyl synthase domain to mimic the sequence of one of the FASs engineered with a cysteine residue at position -3. A helical structure of the N-terminal peptide region was assumed based on a survey of the protein 3D database for similar sequences. 2-propanone was modeled in CS Chem 3D Pro, v.5.0 (CambridgeSoft Corp.), coordinates were transformed into pdb format, and a crosslinker was built into the model of the MACAR  $\beta$ -ketoacyl synthase dimer.

ing the  $\beta$ -ketoacyl synthase domain is entirely monomeric (this report); (iv) the partial FAS construct containing residues 1–971, which lacks the central core region that is thought to play an important role in dimer-

ization, is capable of forming dimers that can reversibly dissociate into monomers under the same conditions as whole FAS (this report); (v) crosslinking studies reveal that the two N termini of FAS subunits are in close proximity in the FAS dimer (this report); (vi) electron microscope images of N-His<sub>6</sub>-tagged FAS with Ni-NTA nanogold show two distinct nanogold clusters located near the center of the structure, not at opposite poles as would be predicted by the head-to-tail model (F.J.A. et al., unpublished data).

All of the data summarized above, together with the homology modeling of the dimeric  $\beta$ -ketoacyl synthase domains, are consistent with the revised model we proposed earlier (Figure 1B).

Clearly, dimeric N-terminal  $\beta$ -ketoacyl synthase domains cannot be accommodated by the head-to-tail model (Figure 1A), which predicts that the N-terminal  $\beta$ -ketoacyl synthase domains are distantly located at opposite poles of the  $\sim$ 180 Å-long dimer [29], where they could not be ligated by crosslinkers with a range of only  $\sim$ 6 Å. On the other hand, the new data are entirely compatible with the alternative model (Figure 1B) that predicted that the two  $\beta$ -ketoacyl synthase domains likely are located close together [5, 7]. Thus, the two polypeptides are orientated head-to-head and not head-to-tail. Since the  $\beta$ -ketoacyl synthase and the malonyl/ acetyl transferase domains located at the N terminus can interact functionally with the ACP domains of either subunit, the head-to-head juxtaposition does not imply that the polypeptides lie side-by-side in a parallel orientation. Rather, they must be coiled so as to permit the full range of functional interactions defined by earlier mutant complementation studies. The challenge ahead is to generate a more detailed map of the topographical features of the FAS complex that will reveal exactly how the two subunits interact both structurally and functionally. We are presently pursuing a combination of chemical crosslinking and structural analysis by single-particle electron microscopy to address this task.

## Significance

The current textbook models for the animal FAS are based on the premise that the two subunits are arranged in a fully extended, antiparallel orientation—the “head-to-tail model” [30]. There is now extensive biochemical evidence that calls into question this view of the complex, and the cornerstone of the model, the assumption that the  $\beta$ -ketoacyl synthase active site cysteine and the ACP phosphopantetheine thiols can be crosslinked *exclusively* between subunits, has proven to be incorrect, as the two thiols can also be crosslinked within the same subunit [6]. The original model also precluded the possibility that the two N-terminal  $\beta$ -ketoacyl synthase domains could engage in homodimeric interactions, since these domains were predicted to lie far apart at opposite poles of the dimer. The results of the present study, together with previously obtained experimental data from our laboratory, provide a compelling argument that the two  $\beta$ -ketoacyl synthase domains in fact lie close together and are likely to form a homodimer. Thus, the type I and

type II  $\beta$ -ketoacyl synthases likely share a similar quaternary structure. The animal FAS has served as a paradigm for understanding the structural organization and operation of the modular polyketide synthases. These large multienzymes are designed with the same basic domain architecture as the FAS, and they indeed resemble multiple FAS ensembles, each of which catalyzes a single chain-extension step, together with a series of  $\beta$ -carbon processing reactions. These polyketide synthases also function as dimeric modules [31], and it has been postulated that the  $\beta$ -ketoacyl synthase domains may themselves be dimeric [32]. The definitive experimental demonstration of the proximity of the  $\beta$ -ketoacyl synthase domains in the FAS dimer lends support to this view.

## Experimental Procedures

### Engineering and Expression of Constructs Encoding FAS and Its Various Subfragments

The general strategies for cDNA construction, baculoviral expression in Sf9 cells, and purification of FASs have been described previously [6, 26, 28, 33–35]. Details of the procedures used to engineer the various modified and truncated FASs used in this study are available as [Supplemental Data](#).

### Dissociation and Reassociation of the 1–971 Fragment of FAS

The purified 1–971 FAS was diluted with water to give 20–25 mM sodium phosphate (pH 7.3) and 1% glycerol; DTT was added to a final concentration of 1 mM, and the protein was stored at 4°C for 8 days. Oligomeric status was monitored by size-exclusion chromatography on a BioSep-SEC-S 3000 column, 300  $\times$  7.8 mm, (Phenomenex), equilibrated and eluted with either 100 or 200 mM sodium phosphate buffer (pH 7.3) containing 1 mM DTT at a flow rate of 1 ml/min at 20°C. Reassociation was performed by restoring the sodium phosphate buffer and glycerol to 0.2 M and 10%, respectively, followed by incubation at 30°C for 60 min. The reassociated (dimeric) form of 1–971 FAS was further purified by size-exclusion chromatography.

### Crosslinking of FAS

The storage buffer of FAS preparations was replaced with 0.2 M sodium phosphate (pH 7), containing 1 mM Tri(2-carboxyethyl)phosphine hydrochloride, and 10% glycerol by repeated centrifugal ultrafiltration in MWCO-100 kDa units until the solution contained below 0.5% storage buffer. FAS preparations, 0.5 mg/ml, were crosslinked with bis-maleimido crosslinkers in the presence of 0.2 mM acetyl-CoA for 30 min at room temperature. Stock solutions of bis-maleimido crosslinkers (Pierce Chemical Co.) were made in dimethylformamide. The solvent concentration was kept below 1.5%, and control samples received identical amount of dimethylformamide. Crosslinking with 6- to 7.5-fold excess of DBP, purified by HPLC [36], was done as described previously [6], except that reactions were carried out for 30 min. Crosslinking reactions were quenched by the addition of mercaptoethanol to 1 mM. Reaction products were analyzed by SDS-PAGE by using a 3% stacking and 4% separating gel and were stained as described [6]. FAS heterodimer was prepared and purified as described previously [7].

### Cleavage by TEV Protease

FAS in 50 mM sodium phosphate (pH 7)/1 mM EDTA/1 mM DTT/10% glycerol was digested with 2 U TEV protease (Invitrogen Corp.) per 1  $\mu$ g FAS for 3 days at room temperature.

### Trypsinization of Crosslinked FAS and Purification of N-Terminal Peptides

Before trypsinization, the pH of crosslinked FAS preparations was adjusted to 8, and acetonitrile was added to 5%. FAS was digested with TPCK-trypsin (Worthington Biochemical Corp.) at a ratio of



2.5:1 at 37°C for 18 hr. Then, 6 M guanidine/0.1 M potassium phosphate (final pH 8) was added to achieve 4 M guanidine concentration; the protein was carboxyamidomethylated with 1.5 mM iodoacetamide for 1 hr, and the reaction was stopped by the addition of mercaptoethanol to 2.5 mM.

His-tagged peptides were purified on Ni-NTA silica spin columns (Qiagen Inc.) according to the manufacturer's recommendations. In brief, the reaction mixture was supplemented with 5 mM imidazole and spun through the column. The column was washed twice with 30 mM imidazole in 3 M guanidine/50 mM potassium phosphate (pH 8), then washed twice with 5 mM ammonium carbonate. Bound peptides were eluted with 0.1% trifluoroacetic acid in 20% acetonitrile and were used directly for mass spectrometric analysis.

#### Identification of Crosslinked Cysteine Peptides by Mass Spectrometry

MALDI-TOF MS analysis of peptide mixtures (in 50% acetonitrile/0.1% TFA) was performed in a water-saturated dihydroxybenzoic acid matrix mixed 1:1 directly on the MALDI target, and the mixtures were allowed to crystallize at room temperature. A Voyager DE STR mass spectrometer (Applied Biosystems) was operated in the positive reflector mode under conditions of external calibration. Instrumental control and data analysis were afforded by Voyager 5.1 and Data Explorer software (Applied Biosystems), respectively. Nano LC ESI MS and MS/MS analysis was performed by utilizing an LC Packings Ultimate HPLC system together with Switchos and Famos Autosampler (LC Packings/Dionex) on-line with a QStar XL, Qq TOF hybrid mass spectrometer (Applied Biosystems/MDX Sciex), equipped with nano-spray ion source (Protana, Odense) and PicoTip Emitter tips (New Objective Inc.). Samples (2–3  $\mu$ l) were desalted on-line by using a Nano-Precolumn (C18, 5  $\mu$ m, 100 Å, 300  $\mu$ m  $\times$  1 mm), and peptides were separated on a PepMap100 column (C18, 3  $\mu$ m, 75  $\mu$ m id, LC Packings/Dionex) by using a gradient of acetonitrile in 0.1% formic acid at a flow rate of 300 nl/min. The instrument was controlled by Analyst software and operated automatically under conditions of external calibration with information-dependent acquisition software (Applied Biosystems/MDX Sciex). Data analysis was performed with Bioanalyst software (Applied Biosystems/MDX Sciex). Deconvolution of MS/MS data to produce zero charge spectra was done by using a Bayesian peptide reconstruction script. Interpretation of MS/MS spectra of crosslinked peptides was aided by MS2Assign software (Sandia National Laboratories, <http://roswell.ca.sandia.gov/~mmyoung>) [37].

#### Enzyme Assays

Overall FAS activity [38] and *trans*-1-decalone reductase activity associated with the  $\beta$ -ketoacyl reductase domain [33] were assessed spectrophotometrically. The acyl transferase activity of the  $\beta$ -ketoacyl synthase domain that is responsible for the translocation of saturated acyl moieties from the phosphopantetheine thiol to the active site Cys161 was assessed at 10°C with model substrates, by monitoring the shuttling of decanoyl moieties from pantetheine and CoA thiols [39]. Activity of the malonyl/acetyl transferase domain was assayed by monitoring the transesterification of [ $^{14}$ C] acetyl moieties from CoA to pantetheine [40]. Dehydrase activity was measured spectrophotometrically [41]. Units of activity are nmol substrate utilized per min.

#### Homology Modeling of $\beta$ -Ketoacyl Synthase Domain

Four X-ray structures of one chain of type II  $\beta$ -ketoacyl synthases, 1kas (*E. coli*, 22% identity, 40% similarity), 1ox0a (*Streptococcus pneumoniae*, 22% identity, 37% similarity), 1j3na (*Thermus thermophilis*, 28% identity, 43% similarity), and 1e5ma (*Synechocystis* Sp., 27% identity, 42% similarity), were used as templates to model the  $\beta$ -ketoacyl synthase domain of rat FAS. A multiple alignment produced by clustalw was submitted to SWISS-MODEL [42, 43]. The model of the dimer was created by superimposing two identical models with the chains A and B of *S. pneumoniae*  $\beta$ -ketoacyl synthase II dimer by using Swiss-PdbViewer, v. 3.7. Clashes were removed by manipulation of side chains, and the model was refined by energy minimization with GROMOS96 implementation of Swiss-PdbViewer. The accuracy of this model depends on the degree of

similarity between the structure of the  $\beta$ -ketoacyl synthase domain of rat FAS and type II  $\beta$ -ketoacyl synthase.

#### Supplemental Data

Supplemental Data including details of the procedures used to engineer, express, and purify the various protein constructs used in this study, together with the mass spectrometric analysis of the peptides derived from dibromopropanone-crosslinked FAS, are available at <http://www.chembiol.com/cgi/content/full/11/12/1667/DC1/>.

#### Acknowledgments

We are grateful to Dr. M.G. Finn of the Scripps Research Institute for his helpful suggestions. The work was supported by grant DK 16073 from the National Institutes of Health to S.S. The Biomolecular Resource Center Mass Spectrometry Laboratory at U.C. San Francisco is supported in part by the Sandler Family Foundation. F.J.A. is a Scholar of the Leukemia and Lymphoma Society of America.

Received: September 8, 2004

Revised: September 25, 2004

Accepted: September 30, 2004

Published: December 17, 2004

#### References

1. Stoops, J.K., and Wakil, S.J. (1981). Animal fatty acid synthetase—a novel arrangement of the  $\beta$ -ketoacyl synthetase sites comprising domains of the two subunits. *J. Biol. Chem.* 256, 5128–5133.
2. Stoops, J.K., and Wakil, S.J. (1982). Animal fatty acid synthetase: identification of the residues comprising the novel arrangement of the  $\beta$ -ketoacyl synthetase site and their role in its cold inactivation. *J. Biol. Chem.* 257, 3230–3235.
3. Wakil, S.J., and Stoops, J.K. (1983). Structure and mechanism of fatty acid synthetase. In *The Enzymes*, P.D. Boyer, ed. (New York: Academic Press), pp. 3–61.
4. Smith, S., Stern, A., Randhawa, Z.I., and Knudsen, J. (1985). Mammalian fatty acid synthetase is a structurally and functionally symmetrical dimer. *Eur. J. Biochem.* 152, 547–555.
5. Rangan, V.S., Joshi, A.K., and Smith, S. (2001). Mapping the functional topology of the animal fatty acid synthase by mutant complementation in vitro. *Biochemistry* 40, 10792–10799.
6. Witkowski, A., Joshi, A.K., Rangan, V.S., Falick, A.M., Witkowska, H.E., and Smith, S. (1999). Dibromopropanone cross-linking of the phosphopantetheine and active-site cysteine thiols of the animal fatty acid synthase can occur both inter- and intra-subunit: re-evaluation of the side-by-side, antiparallel subunit model. *J. Biol. Chem.* 274, 11557–11563.
7. Joshi, A.K., Rangan, V.S., Witkowski, A., and Smith, S. (2003). Engineering of an active animal fatty acid synthase dimer with only one competent subunit. *Chem. Biol.* 10, 169–173.
8. Huang, W., Jia, J., Edwards, P., Dehesh, K., Schneider, G., and Lindqvist, Y. (1998). Crystal structure of  $\beta$ -ketoacyl-acyl carrier protein synthase II from *E. coli* reveals the molecular architecture of condensing enzymes. *EMBO J.* 17, 1183–1191.
9. Moche, M., Schneider, G., Edwards, P., Dehesh, K., and Lindqvist, Y. (1999). Structure of the complex between the antibiotic cerulenin and its target,  $\beta$ -ketoacyl-acyl carrier protein synthase. *J. Biol. Chem.* 274, 6031–6034.
10. Price, A.C., Rock, C.O., and White, S.W. (2003). The 1.3-Å-resolution crystal structure of  $\beta$ -ketoacyl-acyl carrier protein synthase II from *Streptococcus pneumoniae*. *J. Bacteriol.* 185, 4136–4143.
11. Olsen, J.G. (2001). The molecular structure and function of  $\beta$ -ketoacyl synthase I. PhD thesis, University of Copenhagen, Copenhagen, Denmark.
12. Olsen, J.G., Kadziola, A., von Wettstein-Knowles, P., Siggaard-Andersen, M., and Larsen, S. (2001). Structures of  $\beta$ -ketoacyl-

- acyl carrier protein synthase I complexed with fatty acids elucidate its catalytic machinery. *Structure* 9, 233–243.
13. Witkowski, A., Joshi, A.K., and Smith, S. (2002). Mechanism of the  $\beta$ -ketoacyl synthase reaction catalyzed by the animal fatty acid synthase. *Biochemistry* 41, 10877–10887.
  14. Rangan, V.S., Serre, L., Witkowska, H.E., Bari, A., and Smith, S. (1997). Characterization of the malonyl/acetyltransacylase domain of the multifunctional animal fatty acid synthase by expression in *Escherichia coli* and refolding *in vitro*. *Protein Eng.* 10, 561–566.
  15. Smith, S., and Abraham, S. (1971). Fatty acid synthetase from lactating rat mammary gland. III. Dissociation and reassociation. *J. Biol. Chem.* 246, 6428–6435.
  16. Smith, S., Witkowski, A., and Joshi, A.K. (2003). Structural and functional organization of the animal fatty acid synthase. *Prog. Lipid Res.* 42, 289–317.
  17. Kumar, S., Dorsey, J.A., Muesing, R.A., and Porter, J.W. (1970). Comparative studies of the pigeon liver fatty acid synthetase complex and its subunits—kinetics of partial reactions and the number of binding sites for acetyl and malonyl groups. *J. Biol. Chem.* 245, 4732–4744.
  18. Dawson, P.E., Muir, T.W., Clark-Lewis, I., and Kent, S.B. (1994). Synthesis of proteins by native chemical ligation. *Science* 266, 776–779.
  19. Tam, J.P., Lu, Y.A., Liu, C.F., and Shao, J. (1995). Peptide synthesis using unprotected peptides through orthogonal coupling methods. *Proc. Natl. Acad. Sci. USA* 92, 12485–12489.
  20. Green, N.S., Reisler, E., and Houk, K.N. (2001). Quantitative evaluation of the lengths of homobifunctional protein cross-linking reagents used as molecular rulers. *Protein Sci.* 10, 1293–1304.
  21. Garwin, J.L., Klages, A.L., and Cronan, J.E., Jr. (1980). Structural, enzymatic, and genetic studies of  $\beta$ -ketoacyl-acyl carrier protein synthases I and II of *Escherichia coli*. *J. Biol. Chem.* 255, 11949–11956.
  22. Shimakata, T., and Stumpf, P.K. (1982). Purification and characterizations of  $\beta$ -ketoacyl-[acyl-carrier-protein] reductase,  $\beta$ -hydroxyacyl-[acyl-carrier-protein] dehydrase, and enoyl-[acyl-carrier-protein] reductase from *Spinacia oleracea* leaves. *Arch. Biochem. Biophys.* 218, 77–91.
  23. Helmkamp, G.M., Jr., and Bloch, K. (1969).  $\beta$ -hydroxydecanoyl thioester dehydrase. Studies on molecular structure and active site. *J. Biol. Chem.* 243, 6014–6022.
  24. Ruch, F.E., and Vagelos, P.R. (1973). The isolation and general properties of *Escherichia coli* malonyl coenzyme A-acyl carrier protein transacylase. *J. Biol. Chem.* 248, 8086–8094.
  25. Serre, L., Verbree, E.C., Dauter, Z., Stuitje, A.R., and Derewenda, Z.S. (1995). The *Escherichia coli* malonyl-CoA:ACP transacylase at 1.5 Å resolution. *J. Biol. Chem.* 270, 12961–12964.
  26. Joshi, A.K., Witkowski, A., and Smith, S. (1997). Mapping of functional interactions between domains of the animal fatty acid synthase by mutant complementation *in vitro*. *Biochemistry* 36, 2316–2322.
  27. Witkowski, A., Joshi, A.K., Lindqvist, Y., and Smith, S. (1999). Conversion of a  $\beta$ -ketoacyl synthase to a malonyl decarboxylase by replacement of the active-site cysteine with glutamine. *Biochemistry* 38, 11643–11650.
  28. Witkowski, A., Joshi, A.K., and Smith, S. (1996). Fatty acid synthase: *in vitro* complementation of inactive mutants. *Biochemistry* 35, 10569–10575.
  29. Brink, J., Ludtke, S.J., Yang, C.Y., Gu, Z.W., Wakil, S.J., and Chiu, W. (2002). Quaternary structure of human fatty acid synthase by electron cryomicroscopy. *Proc. Natl. Acad. Sci. USA* 99, 138–143.
  30. Voet, D., and Voet, J. (2003). *Biochemistry, Third Edition* (New York: John Wiley & Sons).
  31. Staunton, J., Caffrey, P., Aparicio, J.F., Roberts, G.A., Bethell, S.S., and Leadlay, P.F. (1996). Evidence for a double helical structure for modular polyketide synthases. *Nat. Struct. Biol.* 3, 188–192.
  32. Leadlay, P., and Baerga-Ortiz, A. (2003). Mammalian fatty acid synthase. Closure on a textbook mechanism? *Chem. Biol.* 10, 101–103.
  33. Joshi, A.K., and Smith, S. (1993). Construction of a cDNA encoding the multifunctional animal fatty acid synthase and expression in *Spodoptera frugiperda* cells using baculoviral vectors. *Biochem. J.* 296, 143–149.
  34. Joshi, A.K., and Smith, S. (1993). Construction, expression and characterization of a mutated animal fatty acid synthase deficient in the dehydrase function. *J. Biol. Chem.* 268, 22508–22513.
  35. Joshi, A.K., Rangan, V.S., and Smith, S. (1998). Differential affinity-labeling of the two subunits of the homodimeric animal fatty acid synthase allows isolation of heterodimers consisting of subunits that have been independently modified. *J. Biol. Chem.* 273, 4937–4943.
  36. Witkowski, A., Naggert, J., Witkowska, H.E., Randhawa, Z.I., and Smith, S. (1992). Utilization of an active serine 101  $\rightarrow$  cysteine mutant to demonstrate the proximity of the catalytic serine 101 and histidine 237 residues in thioesterase II. *J. Biol. Chem.* 267, 18488–18492.
  37. Schilling, B., Row, R.H., Gibson, B.W., Guo, X., and Young, M.M. (2003). MS2Assign, automated assignment and nomenclature of tandem mass spectra of chemically crosslinked peptides. *J. Am. Soc. Mass Spectrom.* 14, 834–850.
  38. Smith, S., and Abraham, S. (1975). Fatty acid synthase from lactating rat mammary gland. *Methods Enzymol.* 35, 65–74.
  39. Witkowski, A., Joshi, A.K., and Smith, S. (1997). Characterization of the interthiol acyltransferase reaction catalyzed by the  $\beta$ -ketoacyl synthase domain of the animal fatty acid synthase. *Biochemistry* 36, 16338–16344.
  40. Rangan, V.S., and Smith, S. (1996). Expression in *Escherichia coli* and refolding of the malonyl/acetyl transferase domain of the multifunctional animal fatty acid synthase. *J. Biol. Chem.* 271, 31749–31755.
  41. Witkowski, A., Joshi, A.K., and Smith, S. (2004). Characterization of the  $\beta$ -carbon processing reactions of the mammalian cytosolic fatty acid synthase: role of the central core. *Biochemistry* 43, 10458–10466.
  42. Guex, N., and Peitsch, M.C. (1997). SWISS-MODEL and the Swiss-PdbViewer: an environment for comparative protein modeling. *Electrophoresis* 18, 2714–2723.
  43. Schwede, T., Kopp, J., Guex, N., and Peitsch, M.C. (2003). SWISS-MODEL: an automated protein homology-modeling server. *Nucleic Acids Res.* 31, 3381–3385.
  44. Chirala, S.S., Jayakumar, A., Gu, Z.W., and Wakil, S.J. (2001). Human fatty acid synthase: role of interdomain in the formation of catalytically active synthase dimer. *Proc. Natl. Acad. Sci. USA* 98, 3104–3108.
  45. Roepstorff, P., and Fohlman, J. (1984). Proposal for a common nomenclature for sequence ions in mass spectra of peptides. *Biomed. Mass Spectrom.* 11, 601.